HHS Public Access

Author manuscript

Sci Signal. Author manuscript; available in PMC 2015 April 21.

Published in final edited form as:

Sci Signal. ; 7(329): ra55. doi:10.1126/scisignal.2005169.

A Carma1/MALT1-dependent, Bcl10-independent, pathway regulates antigen receptor-mediated mTOR signaling in T cells

Kristia S. Hamilton[1,2], **Binh Phong**[1,2], **Catherine Corey**[3], **Jing Cheng**[1], **Balachandra Gorentla**[4], **Xiaoping Zhong**[4], **Sruti Shiva**[3], and **Lawrence P. Kane**[1,*]

[1]Department of Immunology, University of Pittsburgh School of Medicine, Pittsburgh, PA 15261, USA.

[2]Graduate Program in Immunology, University of Pittsburgh School of Medicine, Pittsburgh, PA 15261, USA.

[3]Department of Pharmacology and Chemical Biology, University of Pittsburgh School of Medicine, Pittsburgh, PA 15261, USA.

[4]Departments of Pediatrics and Immunology, Duke University Medical Center, Durham, NC 27710, USA.

Abstract

Signaling to the mechanistic target of rapamycin (mTOR) regulates diverse cellular processes, including protein translation, cellular proliferation, metabolism, and autophagy. These effects are mediated in part by the mTOR targets S6 kinase (S6K) and eukaryotic initiation factor 4E (eIF4E)-binding protein 1 (4E-BP1). Most models place Akt upstream of the best-studied mTOR complex, mTORC1; however, studies have called into question whether Akt is necessary for this pathway, at least in T cells. We found that the adaptor protein Carma1 [caspase recruitment domain (CARD)-containing membrane-associated protein 1 (Carma1)] and at least one of its associated proteins, the paracaspase MALT1 (mucosa-associated lymphoid tissue lymphoma translocation protein 1), were required for optimal activation of mTOR in T cells in response to stimulation of the T cell receptor (TCR) and the coreceptor CD28. However, another common binding partner of Carma1 and MALT1, Bcl10, was not required for TCR-dependent activation of the mTOR pathway. Consistent with these findings, MALT1 activity was required for the proliferation of $CD4^+$ T cells, but not early TCR-dependent activation events. Also consistent with an effect on mTOR, MALT1 activity was required for the increased metabolic flux in activated $CD4^+$ T cells. Together, our data suggest that Carma1 and MALT1 play previously unappreciated roles in the activation of mTOR signaling in T cells after engagement of the TCR.

*Corresponding author. lkane@pitt.edu.

Author contributions: K.S.H. designed and performed experiments, analyzed data, and wrote the manuscript; B.P. performed some Western blotting experiments; J.C. generated JPM 50.6 cells reconstituted with Carma1; B.G. and X.Z. performed RT-PCR experiments; C.C. and S.S. performed and analyzed the Seahorse experiments; and L.P.K. conceived of the project and wrote the manuscript.

Competing interests: The authors declare that they have no competing interests.

Introduction

Upon stimulation with antigen, naïve T cells rapidly proliferate, produce cytokines, and migrate from lymphoid organs, after which they mediate diverse effector functions in tissues. Dysregulation of T cell signaling events is associated with autoimmune diseases and lymphomas; thus, dissection of the mechanisms leading to T cell activation may lead to more efficacious therapies. Signaling events initiated by receptors for antigens, growth factors, and cytokines lead to activation of the serine and threonine kinases phosphatidylinositol 3-kinase (PI3K), Akt, and the mechanistic target of rapamycin (mTOR), to regulate cellular growth and proliferation (1, 2). The 70-kD ribosomal protein S6 kinase (p70S6K), which directly phosphorylates ribosomal protein S6, is a key effector of mTOR (3). S6 is a critical regulator of protein translation, because it is necessary for ribosome biogenesis, and is thus an indirect regulator of cellular proliferation (4). Another important substrate of mTOR is the translational inhibitor eukaryotic initiation factor 4E (eIF4E)–binding protein 1 (4E-BP1), phosphorylation of which releases its inhibition of the translation of certain mRNAs (2).

In T cells, engagement of the T cell receptor (TCR) and the co-stimulatory receptor CD28 stimulates activation of PI3K and Akt, which leads to the activation of mTOR, p70S6K, and S6 (5, 6). Investigation of the specific roles of S6K and S6 in the activation of T cells has revealed a requirement for these proteins in cellular proliferation. Notably, heterozygous expression of *Rps6* (the gene encoding S6) limits T cell proliferation in response to stimulation of the TCR, without having any effect on changes in cellular size or on early activation events (7). Akt is a central modulator of T cell signaling pathways that control metabolism, growth, migration, and activation (8-10). However, a study has suggested that the phosphorylation of S6 downstream of the TCR and CD28 is not strictly dependent on Akt (11).

Caspase recruitment domain (CARD)-containing membrane-associated protein 1 (Carma1) is an adaptor protein, predominantly found in lymphocytes, that interacts with B cell lymphoma 10 (Bcl10) and mucosa-associated lymphoid tissue lymphoma translocation protein 1 (MALT1) upon antigen receptor stimulation to form the CBM complex. This protein complex is necessary for optimal activation of the nuclear factor κB (NF-κB) and c-Jun N-terminal kinase (JNK) signaling pathways in response to TCR stimulation (12-15). In addition, both Carma1 and MALT1 act as tumor-promoting proteins in diffuse large B cell lymphoma (DLBCL) (16-19). Studies of the molecular mechanisms by which MALT1 regulates T cell activation have revealed it as a “paracaspase” (20-22). Thus, inhibition of the catalytic activity of MALT1 with the selective inhibitor z-VRPR-fmk leads to partially impaired activation of NF-κB (21).

We have demonstrated previously uncharacterized roles for Carma1 and MALT1 in the activation of T cells, specifically through a signaling pathway leading to the activation of mTORC1. Loss of Carma1 or MALT1 impaired the TCR- and CD28-dependent phosphorylation of S6, as well as of another downstream target of mTOR, 4E-BP1. In contrast, loss of the Carma1- and MALT1-associated protein Bcl10 had no discernible effect on mTORC1 activation. Furthermore, the MALT1 inhibitor z-VRPR-fmk inhibited both the

phosphorylation of S6 and the proliferation of primary $CD4^+$ T cells in response to stimulation of the TCR and CD28. Inhibition of MALT1 activity also impaired the ability of activated T cells to increase their metabolic output, which is largely dependent on the mTOR pathway (23, 24). Thus, our studies have revealed the existence of a previously unappreciated connection between Carma1, MALT1 and mTORC1, which leads to enhanced T cell proliferation and metabolism.

Results

Carma1 is required for the TCR- and CD28-dependent phosphorylation of ribosomal protein S6 in T cells

We previously showed that Akt and Carma1 function cooperatively during T cell activation, specifically through the transcription factor NF-κB (25). To understand other possible downstream effectors of Akt and Carma1, we compared the phosphorylation of potential Akt substrates between the parental human Jurkat T cell lymphoma cell line and a variant cell line lacking Carma1: JPM 50.6 cells (26). We stimulated Jurkat cells, JPM 50.6 cells, and JPM 50.6 transfected with plasmid encoding Carma1 (Carma1-reconstituted JPM 50.6 cells) with anti-CD3 and anti-CD28 antibodies. Through Western blotting analysis with an antibody that recognizes phosphorylated substrates of Akt, we detected a prominent band of about 30 kD with differing patterns of phosphorylation between Jurkat, JPM 50.6, and Carma1-reconstituted JPM 50.6 cells (Fig. 1A). The activation of Akt is normal in JPM 50.6 cells, including both the phosphorylation of Thr^{308} (T308) and Ser^{473} (S473) and its catalytic activity, as shown by us and others (25, 26).

Akt is a member of the large class of AGC kinases, and as such, it shares at least partial substrate specificity (RxRxxS/T) with these kinases, notably the protein kinase p70S6K (R/KxRxxS/T) (27). Based on the mobility of the 30-kD band that we detected (Fig. 1A), we hypothesized that it might be the ribosomal protein S6, a prominent substrate for p70S6K and a downstream effector of the mTOR pathway that is activated by growth factor or TCR signaling (28). Thus, we directly assessed the activation of S6 induced by the TCR and costimulatory molecules through its phosphorylation at Ser^{235} and Ser^{236} (S235/236). Through Western blotting analysis with a phospho-specific antibody, we observed the impaired induction of S6 phosphorylation in Carma1-deficient JPM 50.6 cells compared with that in transfected JPM50.6 cells reconstituted with Carma1 (Fig. 1B). We also observed this defect when S6 phosphorylation was assessed by intracellular phospho-flow cytometry (Fig. 1C, middle panel). However, phosphorylation of S6 in response to amino acids, which proceeds through a distinct pathway (29), was intact in JPM50.6 cells (Fig. 1C, right panel), indicating that the S6 phosphorylation defect in these cells is relatively specific. We also observed apparently identical amounts of total S6 protein in JPM50.6 cells and Jurkat cells (fig. S1A).

Next, we examined the phosphorylation of S6 at an additional cluster of residues, Ser^{240} and Ser^{244} (S240/244), another established readout for S6 activation (4). Again we observed decreased S6 phosphorylation at these sites in JPM 50.6 cells compared with that in the parental Jurkat cells (fig. S1, B and C). For reasons that are unclear, we sometimes observed increased basal phosphorylation of S6 in the JPM 50.6 cells (Fig. 1, B and D). Thus, the

cellular response to amino acid concentrations, which also results in S6K activation and S6 phosphorylation, does not require Carma1. These data suggest that regulation of S6 by Carma1 may be relatively receptor- or cell type–specific.

JPM 50.6 cells were originally derived by chemical mutagenesis of Jurkat cells (26). To further validate the results obtained with these cells, we specifically knocked down Carma1 in Jurkat cells by transducing the cells with lentivirus encoding Carma1-specific short hairpin RNA (shRNA). We then analyzed the phosphorylation of S6 after stimulation of both the parental Jurkat cells and the Carma1 knockdown cells (Carma1shRNA cells) with anti-CD3 and anti-CD28 antibodies. Similar to results obtained with JPM 50.6 cells, we found that the abundance of phosphorylated S6 (pS6) in Carma1shRNA cells was reduced compared to that in parental Jurkat cells transduced with lentivirus encoding control shRNA (Fig. 1D and fig. S1D). To further confirm our findings in primary T cells, we assessed S6 phosphorylation after the stimulation of naïve T cells from wild-type and Carma1 knockout (KO) mice with phorbol 12-myristate 13-acetate (PMA) and ionomycin (30, 31). Consistent with the results obtained from our earlier experiments with cell lines, we observed impaired induction of S6 phosphorylation in the Carma1 KO T cells (Fig. 1E). Together, these data suggest that Carma1 has a previously unrecognized role in TCR signaling events that lead to the phosphorylation of ribosomal protein S6.

Carma1 promotes p70S6K activation and 4E-BP1 phosphorylation

To better define the role of Carma1 in mediating phosphorylation of S6 and associated pathways, we assessed the activity of the kinase immediately upstream of S6, p70S6K (S6K). After engagement of TCR and CD28, p70S6K becomes activated and phosphorylates S6, which leads to increased ribosome biogenesis (32). We found that the extent of p70S6K phosphorylation in stimulated JPM 50.6 cells was reduced compared to that in stimulated Carma1-reconstituted JPM 50.6 cells (Fig. 2A). Additionally, we performed in vitro kinase assays with p70S6K isolated from either Jurkat cells or JPM 50.6 cells, together with glutathione-*S*-transferase (GST)-tagged S6 (GST-S6) as a substrate. We observed an increase in p70S6K catalytic activity after stimulation of the parental Jurkat cells, but not Carma1-deficient JPM 50.6 cells (Fig. 2B). Because p70S6K activity can be enhanced by mTOR (33, 34), we decided to investigate this pathway in more detail.

Our initial experiments suggested that activation-associated phosphorylation of mTOR in Jurkat cells and JPM 50.6 cells was similar, although we could only ever achieve modest, if any, inducible phosphorylation of mTOR by stimulation with anti-CD3 and anti-CD28 antibodies (fig. S2A). We also assessed tuberous sclerosis 2 (TSC2), which lies upstream of mTOR, and observed a modest, and inconsistent, stimulation-dependent increase in TSC2 phosphorylation in both JPM50.6 cells and Carma1-reconstituted JPM 50.6 cells (fig. S2B). We next sought to determine whether other downstream effectors of mTOR, for example 4E-BP1, were regulated by Carma1. Investigation of this pathway in JPM 50.6 cells revealed that these cells had no detectable 4E-BP1 protein, nor did they have mRNA encoding 4E-BP1 (fig. S2, C and D). Thus, we used the Carma1shRNA cells described earlier to determine a possible role for Carma1 in the regulation of 4E-BP1. We observed that the abundance of phosphorylated 4E-BP1 protein in stimulated Carma1shRNA cells

was substantially reduced compared to that in control Jurkat cells, despite both cell types having apparently similar amounts of total 4E-BP1 protein (Fig. 2, C and D). These results suggest that Carma1 also plays a role in the regulation of mTOR activation, upstream of S6K, S6, and 4E-BP1.

PKC activity promotes S6 activation in T cells

Carma1 is "activated" through phosphorylation of its linker domain by multiple isoforms of PKC, among other kinases (35). To assess whether PKC-mediated phosphorylation of Carma1 might play a role in the TCR- and CD28-dependent phosphorylation of S6, we used the well-characterized PKC inhibitor bisindolylmaleimide viii acetate (BIM; fig. S3A). We also used an allosteric Akt-specific inhibitor, Akti1/2 (36), to determine the relative role of Akt in this pathway (fig. S3A). We observed that the TCR- and CD28-dependent phosphorylation of S6 was impaired in D10 cells [a mouse T helper 2 (T_H2) cell line] after these cells were pretreated with BIM or Akti1/2 (Fig. 3A). The latter result is consistent with a report from Macintyre *et al*., who used $CD8^+$ effector T cells (11). Further analysis of the PKC-mediated activation of S6 showed that BIM inhibited S6 phosphorylation in stimulated mouse primary $CD4^+$ T cells (Fig. 3B). To assess a potential requirement for Carma1 in the PKC-mediated phosphorylation of S6, we performed experiments with Jurkat cells or JPM 50.6 cells pre-treated with varying concentrations of BIM. Whereas S6 phosphorylation in parental Jurkat cells was sensitive to BIM, the residual S6 phosphorylation seen in JPM 50.6 cells was refractory to further inhibition by BIM (Fig. 3C). These results are consistent with the existence of a signaling pathway from TCR-mediated activation of PKC to Carma1 and S6 phosphorylation.

MALT1, but not Bcl10, mediates the TCR- and CD28-dependent activation of mTOR signaling

Activation of NF-κB by Carma1 is mediated by at least two other proteins: Bcl10 and MALT1 (37). After engagement of the TCR and CD28, these proteins associate with each other to form the Carma1, Bcl10, and MALT1 (CBM) complex, in which they function to activate downstream effectors, including the inhibitor of κB (IκB) kinase (IKK) complex (38). Thus, we sought to determine whether MALT1 and Bcl10 also played roles in the activation of S6 in experiments with previously described T cell lines that have reduced amounts of Bcl10 or MALT1 as a result of the expression of specific shRNAs (Fig. 4A) (39). Consistent with our earlier findings from experiments with JPM 50.6 and Carma1shRNA cells, we observed impaired phosphorylation of S6 after the TCR- and CD28-dependent stimulation of MALT1shRNA cells compared with that in Bcl10shRNA cells (Fig. 4, B to D). Because of the lack of an apparent effect of loss of Bcl10 on S6 phosphorylation, we next stimulated $CD4^+$ T cells isolated from WT and Bcl10 KO mice and found that both sets of cells were indistinguishable in their ability to induce S6 phosphorylation in response to stimulation (Fig. 4E).

To further investigate a possible requirement for MALT1 in mTOR activation, we also assessed the extent of 4E-BP1 phosphorylation in MALT1shRNA cells. Similar to the phenotype observed in Carma1shRNA cells, 4E-BP1 phosphorylation in cells with reduced MALT1 abundance was substantially reduced compared to that in control Jurkat cells (Fig.

4F and fig. S3B). That S6 phosphorylation was normal in Jurkat cells lacking Bcl10 suggests that the impairment in S6 phosphorylation in Carma1-deficient T cells was not merely a result of dysregulated NF-κB activity. Nonetheless, we confirmed this more directly by assessing the effect of a small-molecule inhibitor of IKK on S6 phosphorylation. As expected, this compound inhibited the activation of an NF-κB reporter in T cells (fig. S3C), but it had no effect on the CD3- and CD28-dependent phosphorylation of S6 in primary T cells (Fig. 4G), indicating that this previously unappreciated pathway was indeed independent of IKK signaling. Thus, these results suggest that whereas MALT1, like Carma1, is required for the optimal phosphorylation of mTOR substrates downstream of TCR and CD28 signaling, Bcl10 does not play as critical a role in this pathway.

To further define the relationship between MALT1 and mTOR-p70S6K signaling, we investigated whether these proteins might be present together in a biochemical complex. We immunoprecipitated MALT1 from T cell lysates and analyzed samples by Western blotting for the presence of p70S6K; MALT1shRNA cells subjected to immunoprecipitation with an anti-MALT1 antibody served as a negative control. Thus, we observed an association between MALT1 and p70S6K in Jurkat cells, which did not seem to depend on stimulation with anti-CD3 and anti-CD28 antibodies (Fig. 4H, left). We were also able to detect the presence of mTOR in a complex with MALT1 (Fig. 4H, right). It is still unclear whether any of these interactions is direct; however, formation of this complex appears to occur independently of TCR signaling, at least in Jurkat cells.

The catalytic activity of MALT1 is required for S6 phosphorylation and cellular proliferation in T cells, but not for early activation events

Selective inhibition of the paracaspase activity of MALT1 with the compound z-VRPR-fmk partially inhibits the activation of NF-κB and retards the growth of activated B cell–like diffuse large B cell lymphoma (ABC DLBCL) cell lines (40). Consistent with earlier studies, we confirmed that this inhibitor partially prevented the TCR- and CD28-dependent, but not the tumor necrosis factor (TNF)-dependent, activation of an NF-κB reporter (fig. S4A). In addition, z-VRPR-fmk had no effect on the phosphorylation of extracellular signal–regulated kinase (ERK) (fig. S4B); however, pretreatment of Jurkat cells with z-VRPR-fmk impaired the activation of the mTOR pathway, as revealed by decreased S6 phosphorylation (Fig. 5A). These results were recapitulated in experiments with primary murine $CD4^+$ T cells, in which pretreatment with z-VRPR-fmk substantially inhibited the anti-CD3– and anti-CD28–dependent phosphorylation of S6 (Fig. 5B). As an additional control for specificity, we also assessed whether z-VRPR-fmk had any effects in MALT1-deficient T cells. Thus, we found that the residual S6 phosphorylation observed in MALT1-deficient T cells was not affected by z-VRPR-fmk (fig. S4C). We also assessed the effects of the MALT1 inhibitor at later time points, and found that z-VRPR-fmk–treated primary $CD4^+$ T cells still had substantially impaired S6 phosphorylation up to 72 hours after stimulation with anti-CD3 and anti-CD28 antibodies (Fig. 5C). These results suggest a specific role for the catalytic activity of MALT1, in addition to its presence, in promoting mTOR activation in T cells.

Previous studies on the functions of Carma1, Bcl10, and MALT1 in T cell activation have predominantly focused on regulation of the transcription factor NF-κB (26, 37, 41). Because our data indicated a requirement for Carma1 and MALT1 for optimal mTOR activation upon T cell stimulation, we next sought to investigate the functional consequences of this pathway. Heterozygous expression of *Rps6* (the gene encoding ribosomal protein S6) results in the impaired proliferation of T cells, but not in the acute increase in cell size ("blasting") that follows T cell activation (7). Based on the role of MALT1 in S6 phosphorylation that we uncovered, we hypothesized that treatment of naïve T cells with the MALT1 inhibitor might phenocopy the effects of reduced S6 abundance on T cell proliferation. We pretreated naïve $CD4^+$ T cells with z-VRPR-fmk and then stimulated them with anti-CD3 and anti-CD28 antibodies for up to 72 hours before assessing cell number, cell size, and activation markers. As we expected, there was an initial decrease in T cell numbers, as a result of the cell death induced by the strong polyclonal anti-CD3 stimulation (Fig. 6A). Although this trend was eventually reversed by 72 hours in the vehicle-treated T cells, because of T cell proliferation, this reversal was not observed in cells treated with z-VRPR-fmk.

We also assessed the effects of z-VRPR-fmk on T cell proliferation more directly, using an assay that measuring reduction of the dye 3-(4,5-dimethylthiazol-2-yl)-2,5-diphenyltetrazolium bromide (MTT). Here, T cell stimulation was performed in the presence of exogenous IL-2 to ensure that the reduction in cell numbers was not a result of the reduced autocrine production of IL-2, as might be expected to happen because of the partial inhibition of NF-κB by z-VRPR-fmk. Thus, z-VRPR-fmk substantially impaired the proliferation of primary $CD4^+$ T cells, even in the presence of exogenous IL-2 (Fig. 6B). Because IL-2 can also promote phosphorylation of S6 through the mTOR pathway (42), this suggests the existence of a nonredundant TCR- and CD28-dependent pathway that requires the catalytic activity of MALT1. Consistent with previous findings on the function of S6 (7), we saw that the decreased number of z-VRPR-fmk–treated cells was not reflected in altered T cell blasting. Thus, cell size, as measured by flow cytometric analysis of forward light scattering, was similar between vehicle- and inhibitor-treated T cells (Fig. 6C). The initial activation of z-VRPR-fmk–treated T cells was comparable to that of vehicle-treated T cells, as determined by flow cytometric analysis of the abundance of the early activation marker CD69 (Fig. 6D). Thus, our data suggest not only that Carma1 and MALT1 are required for the phosphorylation of S6 and its upstream regulator S6K, but also that this pathway controls a known downstream target of S6 in T cells, namely cellular proliferation, whereas it is dispensable for early activation events.

MALT1 promotes the metabolic switch in activated T cells

Naïve T cells are relatively quiescent with respect to cellular metabolism. Upon activation through the TCR, T cells undergo substantial transcriptional and posttranscriptional metabolic reprogramming, which is important for T cell proliferation and differentiation (43, 44). The mTOR pathway is a critical regulator of this increase in cellular metabolism when T cells change from being quiescent to becoming activated (23, 24, 45). Because our data revealed a role for MALT1 in the regulation of both proliferation and the mTOR pathway, we wanted to further assess the functional consequences of this effect. To this end, we assessed the extent of oxidative phosphorylation in $CD4^+$ T cells stimulated overnight in the

presence of the MALT1 inhibitor z-VRPR-fmk or the mTORC1 inhibitor rapamycin. These experiments were carried out in a Seahorse metabolic flux analyzer, which performs real-time measurements of oxidative phosphorylation and glycolysis. As expected, we observed a substantial increase in oxygen consumption in stimulated T cells compared with that in naïve T cells (Fig. 7A). Treatment with z-VRPR-fmk or rapamycin inhibited the shift to increased metabolic activity (Fig. 7A). This effect was apparent both in the basal state and after treatment with carbonyl cyanide-4-(trifluoromethoxy)phenylhydrazone (FCCP), an ionophore uncoupler that promotes the leakage of protons across the inner mitochondrial membrane, and induces maximal oxygen consumption (Fig. 7A). We also assessed the role of MALT1 in the increased extent of aerobic glycolysis, as determined by the extracellular acidification rate (ECAR). As expected, stimulation of naïve T cells markedly increased the extent of glycolysis (Fig. 7B). z-VRPR-fmk partially inhibited glycolysis in stimulated T cells, though not to the same extent as did rapamycin (Fig. 7B); however, this effect was not statistically significant. Increased cell-surface abundance of the amino acid transporter CD98 and CD71 (transferrin receptor) in activated T cells are considered mTOR-dependent events (56); however, we noted no difference in the abundances of these markers between z-VRPR-fmk–treated T cells and vehicle-treated T cells (fig. S4D). Consistent with our earlier data, cells under all conditions exhibited similar cell-surface amounts of CD69, indicative of the efficiency of early TCR-mediated activation, regardless of the presence of the MALT1 inhibitor (Fig. 7C). Thus, inhibition of the protease activity of MALT1 had selective effects during the activation of naïve T cells, in particular on the metabolic reprogramming that is important for the proliferation of T cells.

Discussion

It was previously thought that the phosphorylation of S6 downstream of activation of the TCR and CD28 proceeds exclusively through Akt, the TSC1-TSC2 complex, mTOR, and p70S6K (32), similar to the activation of S6 in other cell types, for example, in response to growth receptor stimulation. However, studies have introduced additional complexity to this simple linear model, specifically with regard to the requirement for Akt, as was demonstrated in experiments with $CD8^+$ T cells (11). Here, we revealed a previously unappreciated role for the proteins Carma1 and MALT1 in signaling upstream of mTOR, resulting in the phosphorylation of the ribosomal protein S6 and the translational regulator 4E-BP1 during T cell activation. This pathway appears to require PKC to a much greater extent than it requires Akt. Whereas we uncovered previously uncharacterized roles for Carma1 and MALT1, we found that Bcl10 was dispensable for S6 activation in T cells. Although most studies indicate that Carma1 and Bcl10 act in concert to mediate T cell activation, Carma1 also disassociates from Bcl10 and binds to other proteins, for example the motor protein guanylate kinase associated kinesin (GAKIN), upon TCR engagement (46).

Our results suggest that Carma1 and MALT1 are also required for the phosphorylation of another target of mTOR signaling, 4E-BP1. Thus, we present a model whereby Carma1 and MALT1 mediate the activation of mTORC1 and its major downstream targets p70S6K and 4E-BP1 (Fig. 8). We found that MALT1 physically associated with both p70S6K and mTOR, consistent with its apparent role in mediating this signaling pathway in T cells,

although it is not clear whether either of these interactions is direct. Whereas mTOR is found in two distinct protein complexes (mTORC1and mTORC2), we hypothesize that MALT1 specifically associates with and regulates mTORC1, because the phosphorylation of Akt at Ser^{473}, a direct target of mTORC2, is normal in Carma1-deficient T cells (25, 26, 28). Additionally, the phosphorylation of Akt at both Thr^{308} and Ser^{473}, as well as the phosphorylation by Akt of one of its direct targets, glycogen synthase kinase 3 beta (GSK3β), is also normal in Carma1-deficient T cells (25, 26). We propose a model whereby, upon stimulation of the TCR and CD28, Carma1 and MALT1 activate mTORC1 and its downstream targets S6 and 4E-BP1, and that this process occurs either downstream of, or parallel to, the Akt-dependent activation of mTORC1. Further study will be necessary to fully understand the underlying molecular mechanism(s) of this previously unappreciated pathway.

Given the known role of the CBM complex in the NF-κB pathway, we considered the possibility that impaired activation of mTOR in Carma1- or MALT1-deficient T cells (or in z-VRPR-fmk– treated T cells) might be a secondary effect of decreased NF-κB activity. However, a small molecule IKK inhibitor did not impair S6 phosphorylation in stimulated primary $CD4^+$ T cells, suggesting that the ability of Carma1 and MALT1 to mediate stimulation of p70S6K and S6 activity is independent of their roles in stimulating NF-κB activation. Regulation of NF-κB by the CBM complex also occurs in other cell types, for example monocytes, in which the Carma1 homolog CARD9 promotes activation of NF-κB (47). Knowing that these proteins have similar functions in other cell types, we are interested in determining whether they might also regulate activation of mTOR signaling.

We often noted increased basal phosphorylation of S6 in Carma1-deficient Jurkat T cells compared to that in the parental cell line, which may be a result of the persistent inhibition of basal S6-mediated protein translation, because this activates p70S6K, and thus S6 (48). Nonetheless, our use of extended nutrient starvation and investigation into additional S6 phosphorylation sites, including S240 and S244, which are indicative of activation (fig. S1B), confirmed our findings that Carma1 mediates the TCR- and CD28-dependent activation of mTOR. Furthermore, T cells from Carma1 KO mice did not exhibit increased basal S6 phosphorylation compared to that in wild type cells (Fig. 1E). Finally, treatment of primary T cells with the MALT1 inhibitor z-VRPR-fmk did not result in increased basal S6 phosphorylation, although it substantially impaired CD3- and CD28-dependent S6 phosphorylation.

The MALT1 inhibitor z-VRPR-fmk partially decreases NF-κB activation in lymphocytes (21). This compound specifically inhibits the paracaspase activity of MALT1 (while not inhibiting classical caspases), and has provided evidence for the catalytic activity of MALT1, which was previously thought to act solely as an adaptor protein (37). Our data provide evidence that suggests another function for MALT1 catalytic activity: the activation of mTORC1. Our data showing normal ERK phosphorylation and increased CD69 abundance in z-VRPR–treated cells suggest that this inhibitor does not have nonspecific effects on T cell activation. In addition, we observed no effects of the inhibitor on residual mTOR activation in MALT1-deficient T cells. Furthermore, several studies from the Thome group have reinforced the specificity of z-VRPR for MALT1 (21, 40, 49).

The mechanism by which the catalytic activity of MALT1 stimulates activation of the signaling pathway that we have characterized here is still unclear, but we hypothesize that there might be additional intermediary molecules that lead to the activation of the mTOR pathway in response to engagement of the TCR and CD28. For example, Kawadler *et al*. demonstrated the MALT1-mediated cleavage of caspase 8, which leads to lymphocyte proliferation (50). Because caspase 8 may also be important for p70S6K activity (51), caspase 8 is another potential link between MALT1 and p70S6K activation. In addition, MALT1-mediated cleavage of the proteins A20 and cylindromatosis (CYLD) are implicated in stimulating NF-κB signaling (20, 52), although neither protein has been implicated in mTOR regulation. A study showed that MALT1 can cleave the protein Regnase-1 (also known as MCPIP1), which normally functions to restrain T cell activation through the destabilization of specific mRNAs, including those that encoding several cytokines (53). Finally, although MALT1 cleaves Bcl10 close to its C-terminus, this event appears to promote lymphocyte adhesion, but not NF-κB activation (21). Thus, MALT1 is not an exclusive stimulator of NF-κB signaling, but participates in other pathways as well.

The major functional connections that we have been able to make thus far between the MALT1-mTOR pathway involve regulation of T cell proliferation and metabolism, but not early activation. The former result is consistent with the finding that primary mouse T cells that have reduced S6 abundance exhibit decreased cellular proliferation, but normal blasting (7). We also showed that MALT1 activity was dispensable for the CD3- and CD28-stimulated blasting of naïve T cells, as well as for the increased abundance of early activation markers, such as CD69. Thus, there may be a distinction between the homeostatic control of cell size, which appears to require Akt and mTOR signaling (54-56), and the more acute, activation-induced increase in cell size that accompanies the proliferation of T cells. The ribosomal protein S6 is a critical regulator of protein translation. It is also one of the main downstream effectors of mTORC1, and as such it is thought to play a critical role in oncogenesis involving defects within the mTOR signaling cascade (57-59). Possible contributions of MALT1 to these pathways will be investigated in future studies.

Our data have also revealed a role for MALT1 in stimulating increased metabolism upon T cell activation, a process important for T cells to meet the changing needs of activated and proliferating T cells (43). The mTOR pathway is an important regulator of this change (45). Based on our study, we propose that the regulation of metabolism in T cells by MALT1 occurs, at least in part, through mTOR. We also assessed the cell-surface abundance of CD71 and CD98, nutrient receptors that facilitate the proliferation of T cells upon activation (60). We observed the increased abundance of both cell-surface markers after stimulation; however treatment with the MALT1 inhibitor did not impair this increase (fig. S4C). These data, together with results from our glycolysis experiments (Fig. 7B), suggest that the MALT1 inhibitor z-VRPR-fmk does not completely inhibit mTOR activation and, thus, we would not expect to see as potent an effect as that seen with the more direct mTOR inhibitor rapamycin (Fig. 7). Numerous reports have described additional important functions for mTOR signaling pathways in the regulation of peripheral T cell differentiation to different effector or regulatory lineages, as well as the regulation of memory T cell development (61, 62). For example, mTORC1 promotes the development of pro-inflammatory T_H17 cells,

whereas it suppresses the development of anti-inflammatory regulatory T cells. Such effects of mTOR in T cells appear to be mediated, at least in part, through regulation of the metabolic reprogramming that accompanies the activation and proliferation of T cells (63). Further study of these aspects of mTOR function is therefore warranted, as possible additional downstream consequences of signaling from Carma1 and MALT1.

Materials and Methods

Mice

C57BL/6 mice were obtained from the Jackson Laboratory. Spleens from Carma1 KO mice were a gift from X. Lin (MD Anderson). Spleens from Bcl10 KO mice were a gift from L. McAllister-Lucas (University of Pittsburgh). Experimental protocols were approved by the Institutional Animal Care and Use Committee (IACUC) at the University of Pittsburgh.

Cell purification

$CD4^+$ T cells were separated by MACS beads (Miltenyi Biotech) according to the manufacturer's protocol. The purity of the final cell population was >90%.

Antibodies and reagents

Phospho-specific antibodies against ribosomal protein S6 (S235/236 and S240/244), p70 ribosomal protein S6K (T389), mTOR (S2448), PKCθ (T538), 4E-BP1 (T70), and phosphorylated substrates of Akt, and Alexa Fluor 647–conjugated antibody against S6 (S235/236 and S240/244) were obtained from Cell Signaling Technology, Inc. Antibodies against ribosomal protein S6, 4E-BP1, and mTOR were also obtained from Cell Signaling Technology, Inc. Antibodies specific for phosphorylated ERK1/2 (T202/Y204) were from BD Biosciences. Antibodies specific for MALT1, p70 S6K, and Bcl10 were from Santa Cruz Biotechnology. Anti-Carma1 antibody was obtained from ProSci Incorporated, whereas the anti– β-actin antibody was from Sigma. Stimulating antibodies, mouse anti-human CD28, hamster anti-mouse CD3 and CD28, phycoerythrin (PE)-conjugated anti-CD69, and phospho-specific antibody against Akt (S473) were obtained from Life Technologies. Fluorescein isothiocyanate (FITC)-conjugated anti-mouse CD71 and PE-conjugated anti-mouse CD98 antibodies were obtained from BioLegend. Horseradish peroxidase (HRP)-conjugated Protein A was from GE Healthcare. Antibody specific to the Jurkat cell TCR (C305) was purified from the C305.2 hybridoma (ATCC). Biotin-conjugated anti-mouse CD3, CD4, and CD28 antibodies were obtained from BD Biosciences. Anti-CD3 and anti-CD28 stimulating antibodies, rabbit anti-Syrian hamster immunoglobulin G (IgG), and the HRP-conjugated donkey anti-rabbit secondary antibody were obtained from Jackson ImmunoResearch Laboratories Inc. The MALT1 inhibitor z-VRPR-fmk was obtained from A.G. Scientific. Recombinant human TNF-α protein was obtained from R&D Systems. PMA, ionomycin, rapamycin, Akt Inhibitor VII (Akti1/2), and IKK inhibitor II (wedelolactone) were obtained from Calbiochem/EMD. Bisindolylmaleimide VIII acetate was from Enzo Life Sciences. Minimum essential media (MEM) amino acid solution was from Hyclone.

Cells

Jurkat cells, Jurkat cell mutants, including JPM 50.6 cells, MALT1shRNA cells, Bcl10shRNA cells, Carma1shRNA cells, Control shRNA cells, and Carma1-reconstituted JPM 50.6 cells, as well as D10 cells (a mouse T cell clone) were maintained as previously described (39, 64, 65). HEK 293T cells were maintained in DMEM, supplemented with 10% bovine growth serum, penicillin/streptomycin and glutamine.

Flow cytometric analysis

Flow cytometric analysis was performed as previously described (65). Briefly, cells were starved of serum in phosphate-buffered saline (PBS), 1% bovine serum albumin (BSA) for 1 hour at 37°C. Where indicated in the figure legends, cells were also pretreated with the appropriate inhibitors during the starvation period. After stimulation, cells were fixed with 1.5% paraformaldehyde at room temperature and were permeablized with cold methanol on ice. Cells were then washed three times and incubated with phospho-specific antibodies at room temperature. Samples were processed on a BD LSRII flow cytometer and data were analyzed with FlowJo software. Where indicated, “fold increase” is defined as the mean fluorescence intensity (MFI) of stimulated cells, divided by that of unstimulated cells.

Luciferase assays

Jurkat cells were transfected with 15 μg of NF-κB luciferase reporter plasmid by electroporation, and then were cultured in complete medium (RPMI, 5% bovine growth serum (BGS), containing penicillin and streptomycin) for 16 to 20 hours. Cells were pretreated with vehicle or inhibitor before being stimulated for 6 hours, with anti-CD3 and anti-CD28 antibodies, PMA and ionomycin, or recombinant human TNF-α. Luciferase assays were performed as previously described (25).

Western blotting analysis and immunoprecipitations

Cells were lysed in NP-40 lysis buffer [1% NP-40, 1 mM EDTA, 20 mM Tris-HCl (pH X.X), 150 mM NaCl] or with radioimmunoprecipitation assay (RIPA) buffer [1% NP-40, 150 mM NaCl, 25 mM Tris-HCl (pH 7.6), sodium deoxycholate, SDS] for immunoprecipitation (IP) before being used for kinase assays. IP's were carried out with 20 ul of a 50% slurry of protein G-agarose beads (Millipore). Proteins were resolved by 8 to 10% SDS-polyacrylamide gel electrophoresis (SDS-PAGE) and were transferred to polyvinylidene difluoride (PVDF) membranes, which were then blocked in 4% BSA. Membranes were then incubated with the primary antibodies specified in the figure legends, followed by HRP-conjugated secondary antibodies. Proteins were detected with the SuperSignal West Pico ECL substrate (Thermo Scientific) and imaged on a Kodak Image Station. β-actin was used as a loading control for Western blotting analysis.

In vitro kinase assays

S6K was immunoprecipitated from stimulated Jurkat cells with a specific antibody and protein G beads, and immunoprecipitates were washed with kinase buffer [50 mM Hepes (pH 7.4), 200mM NaCl, 1% NP-40, and 1 mM EDTA]. After washing, protein G beads were

incubated for 30 min at 30°C in kinase reaction mix (kinase buffer, GST-S6, and γ-^{32}P-ATP), and reactions were stopped with 2× Laemmli sample buffer (Bio-Rad).

Lentiviral transduction and generation of stable cell lines

HEK 293T cells were co-transfected with the pLKO.1 lentiviral vector or the pLEX vector encoding shRNA specific for human Carma1, together with the psPAX2 packaging plasmid and the pMO2.G envelope plasmid with Effectene reagent (Qiagen). Virus-containing culture medium was collected by centrifugation 48 hours later, and was used to generate stable cell lines. Jurkat cells were cultured with virus-containing medium and complete medium in a 1:1 ratio, which was replaced with complete medium 24 hours later. To generate cell lines expressing control shRNA, Jurkat cells were transiently transfected with a pCMV-XL6 plasmid encoding a control shRNA and placed in selection medium 2 days later. Seeding and selection of positive clones with puromycin (for Carma1shRNA and Carma1-reconstituted JPM 50.6 cells) or G418 (for cell lines expressing control shRNA) was performed as previously described (66).

Cell number and MTT proliferation assays

The number of viable CD4+ T cells was determined by manual counting and trypan blue exclusion. Primary T cell proliferation was assessed with the Cell Titer 96 Aqueous Non-Radioactive Cell Proliferation Assay (Promega). $CD4^+$ T cells were stimulated with anti-CD3 and anti-CD28 antibodies for the times indicated in the figures, and cells were collected and incubated with substrate for 24 hours at 37°C in a humidified, 5% CO_2 atmosphere. Absorbance was recorded at 490 nm on an ELISA plate reader.

Seahorse analysis of T cell respiration

Naïve $CD4^+$ T cells were isolated from C57BL/6 mice, pretreated with z-VRPR-fmk or rapamycin, where indicated, and stimulated for 24 hours in a XF24 cell culture microplate (Seahorse Bioscience). Cells were then analyzed with the Seahorse XF24 Extracellular Flux Analyzer (Seahorse Bioscience) as previously described (67).

Real-time PCR

RNAs extracted with Trizol Reagent (Invitrogen) were reverse-transcribed to generate complementary DNA (cDNA) with Superscript III and random primers. Quantitative real-time polymerase chain reaction (qRT-PCR) assays was performed with Mastercycler realplex and SYBR Green master mix (Eppendorf). The abundance of *EIF4EBP1* mRNA (encoding 4E-BP1) was normalized to that of *ACTB* mRNA (encoding β-actin), as calculated with the $2^{-\Delta\Delta CT}$ method. The primers used were as follows: *EIF4EBP1* forward: 5'-GCGCAATAGCCCAGAAGATA-3'; *EIF4EBP1* 1 reverse: 5'-CCCTTGGTAGTGCTCCACAC-3'; β-actin forward: 5'-TGTCCACCTTCCAGCAGATGT-3'; β-actin reverse: 5'-AGCTCAGTAACAGTCCGCCTAGA-3'.

Supplementary Material

Refer to Web version on PubMed Central for supplementary material.

Acknowledgments

We thank J. Ashwell (National Cancer Institute, National Institutes of Health) for the MALTshRNA and Bcl10shRNA cells; J. Blenis (Harvard) for the GST-S6 cDNA; X. Lin and M. Blonska (MD Anderson) for spleens from Carma1 KO mice; and L. McAllister-Lucas and L. Klei (University of Pittsburgh) for spleens from Bcl10 KO mice. We are also grateful to Y. Jiang, P. C. Lucas, and S. Gaffen (University of Pittsburgh) for review of the manuscript and helpful comments. **Funding:** This project was funded by grants from the NIH to L.P.K. (R01GM080398) and to X.Z. (R01AI101206), and by a grant from the Hemophilia Center of Western Pennsylvania to S.S.

References and Notes

1. Sarbassov DD, Ali SM, Sabatini DM. Growing roles for the mTOR pathway. Curr. Opin. Cell Biol. 2005; 17:596–603. [PubMed: 16226444]
2. Laplante M, Sabatini DM. mTOR signaling in growth control and disease. Cell. 2012; 149:274–293. [PubMed: 22500797]
3. Wullschleger S, Loewith R, Hall MN. TOR Signaling in Growth and Metabolism. Cell. 2006; 124:471–484. [PubMed: 16469695]
4. Ruvinsky I, Meyuhas O. Ribosomal protein S6 phosphorylation: from protein synthesis to cell size. Trends in Biochemical Sciences. 2006; 31:342–348. [PubMed: 16679021]
5. Ward G. S. Phosphoinositide 3-Kinases and Leukocyte Migration. Current Immunology Reviews. 8:154–160.
6. Sinclair LV, Finlay D, Feijoo C, Cornish GH, Gray A, Ager A, Okkenhaug K, Hagenbeek TJ, Spits H, Cantrell DA. Phosphatidylinositol-3-OH kinase and nutrient-sensing mTOR pathways control T lymphocyte trafficking. Nat Immunol. 2008; 9:513–521. [PubMed: 18391955]
7. Sulic S, Panic L, Barkic M, Mercep M, Uzelac M, Volarevic S. a. Inactivation of S6 ribosomal protein gene in T lymphocytes activates a p53-dependent checkpoint response. Genes & Development. 2005; 19:3070–3082. [PubMed: 16357222]
8. Cantrell DA. Regulation and function of serine kinase networks in lymphocytes. Current Opinion in Immunology. 2003; 15:294–298. [PubMed: 12787754]
9. Juntilla MM, Koretzky GA. Critical roles of the PI3K/Akt signaling pathway in T cell development. Immunology Letters. 2008; 116:104–110. [PubMed: 18243340]
10. Kane LP, Weiss A. The PI-3 kinase/Akt pathway and T cell activation: pleiotropic pathways downstream of PIP3. Immunological Reviews. 2003; 192:7–20. [PubMed: 12670391]
11. Macintyre AN, Finlay D, Preston G, Sinclair LV, Waugh CM, Tamas P, Feijoo C, Okkenhaug K, Cantrell DA. Protein Kinase B Controls Transcriptional Programs that Direct Cytotoxic T Cell Fate but Is Dispensable for T Cell Metabolism. Immunity. 2011; 34:224–236. [PubMed: 21295499]
12. Blonska M, Pappu BP, Matsumoto R, Li H, Su B, Wang D, Lin X. The CARMA1-Bcl10 Signaling Complex Selectively Regulates JNK2 Kinase in the T Cell Receptor-Signaling Pathway. Immunity. 2007; 26:55–66. [PubMed: 17189706]
13. Che T, You Y, Wang D, Tanner MJ, Dixit VM, Lin X. MALT1/Paracaspase Is a Signaling Component Downstream of CARMA1 and Mediates T Cell Receptor-induced NF-kB Activation. Journal of Biological Chemistry. 2004; 279:15870–15876. [PubMed: 14754896]
14. Gaide O, Favier B, Legler DF, Bonnet D, Brissoni B, Valitutti S, Bron C, Tschopp J, Thome M. CARMA1 is a critical lipid raft-associated regulator of TCR-induced NF-[kappa]B activation. Nature Immunology. 2002; 3:836–843. [PubMed: 12154360]
15. Ruland, J. r.; Duncan, GS.; Elia, A.; del Barco Barrantes, I.; Nguyen, L.; Plyte, S.; Millar, DG.; Bouchard, D.; Wakeham, A.; Ohashi, PS.; Mak, TW. Bcl10 Is a Positive Regulator of Antigen Receptor Induced Activation of NF-k B and Neural Tube Closure. Cell. 2001; 104:33–42. [PubMed: 11163238]
16. Lenz G, Davis RE, Ngo VN, Lam L, George TC, Wright GW, Dave SS, Zhao H, Xu W, Rosenwald A, Ott G, Muller-Hermelink HK, Gascoyne RD, Connors JM, Rimsza LM, Campo E, Jaffe ES, Delabie J, Smeland EB, Fisher RI, Chan WC, Staudt LM. Oncogenic CARD11

Mutations in Human Diffuse Large B Cell Lymphoma. Science. 2008; 319:1676–1679. [PubMed: 18323416]

17. Lenz G, Wright GW, Emre NCT, Kohlhammer H, Dave SS, Davis RE, Carty S, Lam LT, Shaffer AL, Xiao W, Powell J, Rosenwald A, Ott G, Muller-Hermelink HK, Gascoyne RD, Connors JM, Campo E, Jaffe ES, Delabie J, Smeland EB, Rimsza LM, Fisher RI, Weisenburger DD, Chan WC, Staudt LM. Molecular subtypes of diffuse large B-cell lymphoma arise by distinct genetic pathways. Proceedings of the National Academy of Sciences. 2008; 105:13520–13525.
18. Ngo VN, Davis RE, Lamy L, Yu X, Zhao H, Lenz G, Lam LT, Dave S, Yang L, Powell J, Staudt LM. A loss-of-function RNA interference screen for molecular targets in cancer. Nature. 2006; 441:106–110. [PubMed: 16572121]
19. Shaffer AL, Rosenwald A, Staudt LM. Lymphoid Malignancies: the dark side of B-cell differentiation. Nat Rev Immunol. 2002; 2:920–933. [PubMed: 12461565]
20. Coornaert B, Baens M, Heyninck K, Bekaert T, Haegman M, Staal J, Sun L, Chen ZJ, Marynen P, Beyaert R. T cell antigen receptor stimulation induces MALT1 paracaspase-mediated cleavage of the NF-[kappa]B inhibitor A20. Nat Immunol. 2008; 9:263–271. [PubMed: 18223652]
21. Rebeaud F, Hailfinger S, Posevitz-Fejfar A, Tapernoux M, Moser R, Rueda D, Gaide O, Guzzardi M, Iancu EM, Rufer N, Fasel N, Thome M. The proteolytic activity of the paracaspase MALT1 is key in T cell activation. Nat Immunol. 2008; 9:272–281. [PubMed: 18264101]
22. Staal J, Bekaert T, Beyaert R. Regulation of NF-[kappa]B signaling by caspases and MALT1 paracaspase. Cell Res. 2011; 21:40–54. [PubMed: 21119681]
23. Schieke SM, Phillips D, McCoy JP, Aponte AM, Shen R-F, Balaban RS, Finkel T. The Mammalian Target of Rapamycin (mTOR) Pathway Regulates Mitochondrial Oxygen Consumption and Oxidative Capacity. Journal of Biological Chemistry. 2006; 281:27643–27652. [PubMed: 16847060]
24. Yang K, Chi H. mTOR and metabolic pathways in T cell quiescence and functional activation. Seminars in Immunology. 2012; 24:421–428. [PubMed: 23375549]
25. Narayan P, Holt B, Tosti R, Kane L. CARMA1 is required for Akt-Mediated NF-kB Activation in T cells. Molecular Cell Biology. 2006; 26:2327–2336.
26. Wang D, You Y, Case SM, McAllister-Lucas LM, Wang L, DiStefano PS, Nunez G, Bertin J, Lin X. A requirement for CARMA1 in TCR-induced NF-[kappa]B activation. Nature Immunology. 2002; 3:830–835. [PubMed: 12154356]
27. Pearce LR, Komander D, Alessi DR. The nuts and bolts of AGC protein kinases. Nat Rev Mol Cell Biol. 2010; 11:9–22. [PubMed: 20027184]
28. Laplante M, Sabatini DM. mTOR signaling at a glance. Journal of Cell Science. 2009; 122:3589–3594. [PubMed: 19812304]
29. Tato I, Bartrons R, Ventura F, Rosa JL. Amino Acids Activate Mammalian Target of Rapamycin Complex 2 (mTORC2) via PI3K/Akt Signaling. Journal of Biological Chemistry. 2011; 286:6128–6142. [PubMed: 21131356]
30. Chatila T, Silverman L, Miller R, Geha R. Mechanisms of T cell activation by the calcium ionophore ionomycin. The Journal of Immunology. 1989; 143:1283–1289. [PubMed: 2545785]
31. Hara H, Wada T, Bakal C, Kozieradzki I, Suzuki S, Suzuki N, Nghiem M, Griffiths EK, Krawczyk C, Bauer B, D'Acquisto F, Ghosh S, Yeh W-C, Baier G, Rottapel R, Penninger JM. The MAGUK Family Protein CARD11 Is Essential for Lymphocyte Activation. Immunity. 2003; 18:763–775. [PubMed: 12818158]
32. Powell JD, Delgoffe GM. The Mammalian Target of Rapamycin: Linking T Cell Differentiation, Function, and Metabolism. Immunity. 2010; 33:301–311. [PubMed: 20870173]
33. Mondino A, Mueller DL. mTOR at the crossroads of T cell proliferation and tolerance. Seminars in Immunology. 2007; 19:162–172. [PubMed: 17383196]
34. Sabatini DM. mTOR and cancer: insights into a complex relationship. Nature Rev. Cancer. 2006; 6:729–734. [PubMed: 16915295]
35. Thome M, Weil R. Post-translational modifications regulate distinct functions of CARMA1 and BCL10. Trends in Immunology. 2007; 28:281–288. [PubMed: 17468049]
36. Barnett SF, Defeo-Jones D, Fu S, Hancock PJ, Haskell KM, Jones RE, Kahana JA, Kral AM, Leander K, Lee LL, Malinowski J, McAvoy EM, Nahas DD, Robinson RG, Huber HE.

Identification and characterization of pleckstrin-homology-domain-dependent and isoenzyme-specific Akt inhibitors. Biochemical Journal. 2005; 385:399–408. [PubMed: 15456405]

37. Thome M. CARMA1, BCL-10 and MALT1 in lymphocyte development and activation. Nat Rev Immunol. 2004; 4:348–359. [PubMed: 15122200]
38. Thome M, Charton JE, Pelzer C, Hailfinger S. Antigen Receptor Signaling to NF-kB via CARMA1, BCL10, and MALT1. Cold Spring Harbor Perspectives in Biology. 2010; 2
39. Wu C-J, Ashwell JD. NEMO recognition of ubiquitinated Bcl10 is required for T cell receptor-mediated NF-kB activation. Proceedings of the National Academy of Sciences. 2008; 105:3023–3028.
40. Hailfinger S, Lenz G, Ngo V, Posvitz-Fejfar A, Rebeaud F, Guzzardi M, Penas E-MM, Dierlamm J, Chan WC, Staudt LM, Thome M. Essential role of MALT1 protease activity in activated B cell-like diffuse large B-cell lymphoma. Proceedings of the National Academy of Sciences. 2009; 106:19946–19951.
41. Sun L, Deng L, Ea C-K, Xia Z-P, Chen ZJ. The TRAF6 Ubiquitin Ligase and TAK1 Kinase Mediate IKK Activation by BCL10 and MALT1 in T Lymphocytes. Molecular Cell. 2004; 14:289–301. [PubMed: 15125833]
42. Evans SW, Farrar WL. Interleukin 2 and diacylglycerol stimulate phosphorylation of 40 S ribosomal S6 protein. Correlation with increased protein synthesis and S6 kinase activation. Journal of Biological Chemistry. 1987; 262:4624–4630. [PubMed: 3494010]
43. Pearce EL. Metabolism in T cell activation and differentiation. Current Opinion in Immunology. 2010; 22:314–320. [PubMed: 20189791]
44. Rathmell JC, Heiden MGV, Harris MH, Frauwirth KA, Thompson CB. In the Absence of Extrinsic Signals, Nutrient Utilization by Lymphocytes Is Insufficient to Maintain Either Cell Size or Viability. Molecular Cell. 2000; 6:683–692. [PubMed: 11030347]
45. Wullschleger S, Loewith R, Hall MN. TOR signaling in growth and metabolism. Cell. 2006; 124:471–484. [PubMed: 16469695]
46. Lamason RL, Kupfer A, Pomerantz JL. The Dynamic Distribution of CARD11 at the Immunological Synapse Is Regulated by the Inhibitory Kinesin GAKIN. Molecular Cell. 2010; 40:798–809. [PubMed: 21145487]
47. Bertin J, Guo Y, Wang L, Srinivasula SM, Jacobson MD, Poyet J-L, Merriam S, Du M-Q, Dyer MJS, Robison KE, DiStefano PS, Alnemri ES. CARD9 Is a Novel Caspase Recruitment Domain-containing Protein That Interacts With BCL10/CLAP and Activates NF-kB. Journal of Biological Chemistry. 2000; 275:41082–41086. [PubMed: 11053425]
48. Zheng X-F, Schreiber SL. Target of rapamycin proteins and their kinase activities are required for meiosis. Proceedings of the National Academy of Sciences. 1997; 94:3070–3075.
49. Hailfinger S, Nogai H, Pelzer C, Jaworski M, Cabalzar K, Charton J-E, Guzzardi M, Dacaillet C, Grau M, Durken B, Lenz P, Lenz G, Thome M. Malt1-dependent RelB cleavage promotes canonical NF-kB activation in lymphocytes and lymphoma cell lines. Proceedings of the National Academy of Sciences. 2011; 108:14596–14601.
50. Kawadler H, Gantz MA, Riley JL, Yang X. The Paracaspase MALT1 Controls Caspase-8 Activation during Lymphocyte Proliferation. Molecular Cell. 2008; 31:415–421. [PubMed: 18691973]
51. Arechiga AF, Bell BD, Leverrier S, Weist BM, Porter M, Wu Z, Kanno Y, Ramos SJ, Ong ST, Siegel R, Walsh CM. A Fas-Associated Death Domain Protein/Caspase-8-Signaling Axis Promotes S-Phase Entry and Maintains S6 Kinase Activity in T Cells Responding to IL-2. J Immunol. 2007; 179:5291–5300. [PubMed: 17911615]
52. Staal J, Driege Y, Bekaert T, Demeyer A, Muyllaert D, Van Damme P, Gevaert K, Beyaert R. T-cell receptor-induced JNK activation requires proteolytic inactivation of CYLD by MALT1. The EMBO journal. 2011; 30:1742–1752. [PubMed: 21448133]
53. Uehata T, Iwasaki H, Vandenbon A, Matsushita K, Hernandez-Cuellar E, Kuniyoshi K, Satoh T, Mino T, Suzuki Y, Standley DM, Tsujimura T, Rakugi H, Isaka Y, Takeuchi O, Akira S. Malt1-induced cleavage of regnase-1 in CD4(+) helper T cells regulates immune activation. Cell. 2013; 153:1036–1049. [PubMed: 23706741]

54. Faridi J, Fawcett J, Wang L, Roth RA. Akt promotes increased mammalian cell size by stimulating protein synthesis and inhibiting protein degradation. American Journal of Physiology - Endocrinology And Metabolism. 2003; 285:E964–E972. [PubMed: 12876075]

55. Fingar DC, Salama S, Tsou C, Harlow E, Blenis J. Mammalian cell size is controlled by mTOR and its downstream targets S6K1 and 4EBP1/eIF4E. Genes & Development. 2002; 16:1472–1487. [PubMed: 12080086]

56. Edinger AL, Thompson CB. Akt Maintains Cell Size and Survival by Increasing mTOR-dependent Nutrient Uptake. Molecular Biology of the Cell. 2002; 13:2276–2288. [PubMed: 12134068]

57. De J, Brown R. Tissue-microarray based immunohistochemical analysis of survival pathways in nodular sclerosing classical Hodgkin lymphoma as compared with Non-Hodgkin's lymphoma. Int J Clin Exp Med. 2010; 3:55–68. [PubMed: 20369041]

58. Pham LV, Tamayo AT, Li C, Bornmann W, Priebe W, Ford RJ. Degrasyn Potentiates the Antitumor Effects of Bortezomib in Mantle Cell Lymphoma Cells In vitro and In vivo: Therapeutic Implications. Molecular Cancer Therapeutics. 2010; 9:2026–2036. [PubMed: 20606045]

59. Witzig TE, Gupta M. Signal Transduction Inhibitor Therapy for Lymphoma. Hematology. 2010; 2010:265–270. [PubMed: 21239804]

60. Kelly AP, Finlay DK, Hinton HJ, Clarke RG, Fiorini E, Radtke F, Cantrell DA. Notch-induced T cell development requires phosphoinositide-dependent kinase 1. The EMBO Journal. 2007; 26:3441–3450. [PubMed: 17599070]

61. Chi H. Regulation and function of mTOR signalling in T cell fate decisions. Nature reviews. Immunology. 2012; 12:325–338.

62. Waickman AT, Powell JD. Mammalian target of rapamycin integrates diverse inputs to guide the outcome of antigen recognition in T cells. Journal of immunology. 2012; 188:4721–4729.

63. Zeng H, Chi H. mTOR and lymphocyte metabolism. Current opinion in immunology. 2013; 25:347–355. [PubMed: 23722114]

64. Cheng J, Phong B, Wilson DC, Hirsch R, Kane LP. Akt fine-tunes NF-kB-dependent gene expression during T cell activation. Journal of Biological Chemistry. 2011

65. Lee J, Su EW, Zhu C, Hainline S, Phuah J, Moroco JA, Smithgall TE, Kuchroo VK, Kane LP. Phosphotyrosine-Dependent Coupling of Tim-3 to T-Cell Receptor Signaling Pathways. Molecular and Cellular Biology. 2011; 31:3963–3974. [PubMed: 21807895]

66. van Meerten T, van Rijn RS, Hol S, Hagenbeek A, Ebeling SB. Complement-Induced Cell Death by Rituximab Depends on CD20 Expression Level and Acts Complementary to Antibody-Dependent Cellular Cytotoxicity. Clinical Cancer Research. 2006; 12:4027–4035. [PubMed: 16818702]

67. Heid ME, Keyel PA, Kamga C, Shiva S, Watkins SC, Salter RD. Mitochondrial Reactive Oxygen Species Induces NLRP3-Dependent Lysosomal Damage and Inflammasome Activation. The Journal of Immunology. 2013; 191:5230–5238. [PubMed: 24089192]

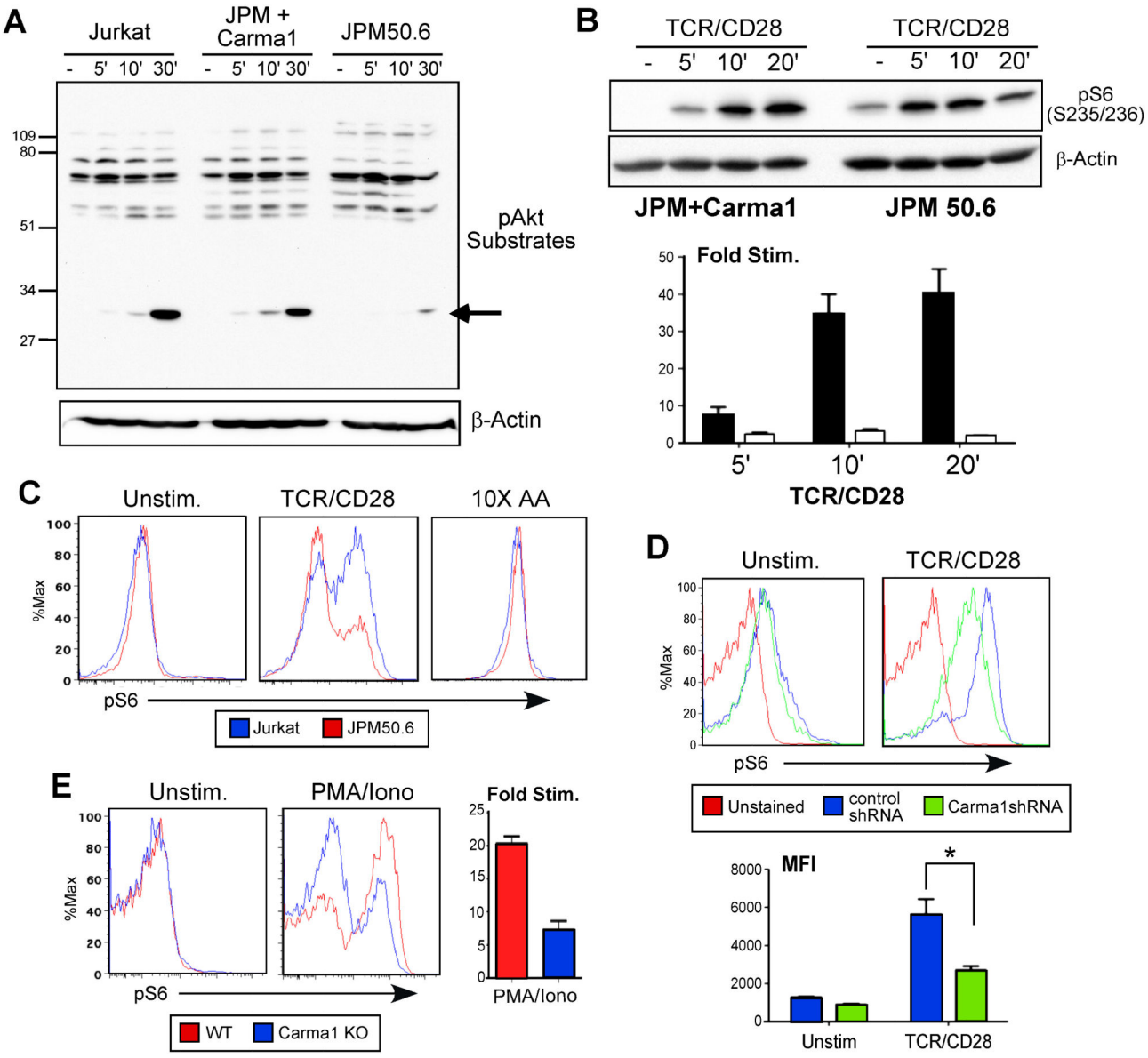

Fig. 1. Carma1 is required for TCR- and CD28-mediated phosphorylation of S6

(**A**) Jurkat cells, JPM 50.6 cells transfected with plasmid encoding Carma1 (JPM + Carma1), and JPM 50.6 cells were left unstimulated or were stimulated with antibodies against CD3 and CD28 (TCR/CD28) for the indicated times and then were analyzed by Western blotting with an antibody specific for phosphorylated substrates of Akt. β-actin was used as a loading control. (**B**) Top: JPM 50.6 cells and Carma1-reconstituted JPM 50.6 cells were left unstimulated or were stimulated with anti-CD3 and anti-CD28 antibodies for the indicated times, and then were analyzed by Western blotting with an antibody specific for S6 phosphorylated at S235/236. β-actin was used as a loading control. Bottom: Quantitation of the fold-increase in the abundance of pS6 protein. Densitometric analysis was used to determine the relative intensities of bands corresponding to pS6, which were normalized to those of β-actin. The relative fold-increases in pS6 abundance in the Carma1-reconstituted JPM 50.6 cells (filled bars) and JPM 50.6 cells (empty bars) at the indicated times were then

calculated, based on three independent experiments. (**C**) Jurkat cells and JPM 50.6 cells were left unstimulated or were stimulated with anti-CD3 and anti-CD28 antibodies or with amino acids (10X AA). Cells were then analyzed by flow cytometry to detect pS6. (**D**) Jurkat cells expressing control shRNA or Carma1-specific shRNA (Carma1shRNA cells) were left unstimulated or were stimulated with anti-CD3 and anti-CD28 antibodies for 15 min before being analyzed by flow cytometry for pS6. The graph below shows mean MFI ± SEM of triplicate samples. (**E**) Primary $CD4^+$ T cells isolated from wild-type (WT) or Carma1 KO mice were left unstimulated or were stimulated with PMA and ionomycin for 15 min before being analyzed by flow cytometry to detect pS6. Data in the bar graph represent mean fold-increases ± SEM in pS6 abundance in duplicate samples of stimulated WT or Carma1 KO T cells, relative to that in unstimulated cells. $*P < 0.05$, $**P < 0.01$ by unpaired student's t test. Data in all panels are representative of three independent experiments.

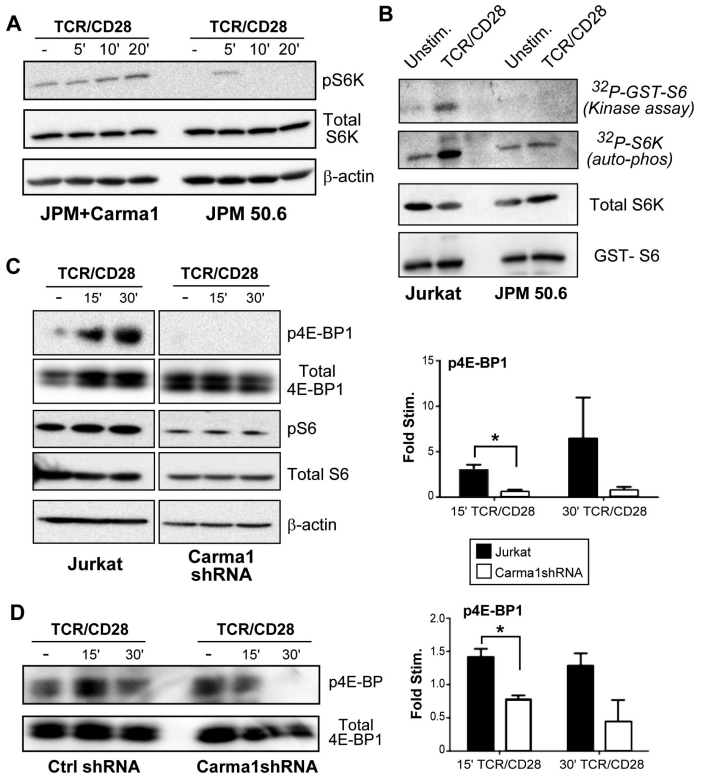

Fig. 2. The phosphorylation of mTOR targets in response to stimulation of TCR and CD28 depends on Carma1

(**A**) JPM 50.6 cells and Carma1-reconstituted JPM 50.6 cells were left untreated or were treated with anti-CD3 and anti-CD28 antibodies (TCR/CD28) for the indicated times before being analyzed by Western blotting with antibodies against the indicated proteins. (**B**) Jurkat cells and JPM 50.6 cells were left untreated or were treated with anti-CD3 and anti-CD28 antibodies for 15 min before being subjected to immunoprecipitation (IP) of S6K with a specific antibody. IP'd samples were analyzed by in vitro kinase assays with GST-S6 as the substrate. Top panels: Reactions were analyzed by autoradiography to examine GST-S6 phosphorylation and S6K auto-phosphorylation. Bottom panels: Reactions were also analyzed by Western blotting to determine the relative amounts of IP'd S6K and GST-S6. Data in panels A and B are representative of three independent experiments. (**C** and **D**) Left: Untransfected Jurkat cells (C) or Jurkat cells transfected with a control shRNA (D) and Carma1shRNA cells (D) were left untreated or were stimulated with anti-CD3 and anti-CD28 antibodies for the indicated times and then were analyzed by Western blotting with antibodies against the indicated proteins. Right: Graphs show the fold-increase in the abundance of p4E-BP1 (normalized to that of total 4E-BP1) in the indicated cells at the indicated times. Data shown are the means ± SEM from three (panel C) or two (panel D) independent experiments.

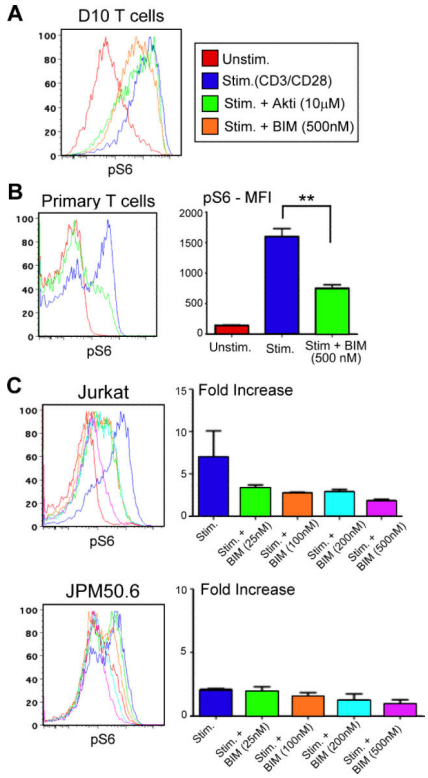

Fig. 3. The TCR- and CD28-stimulated phosphorylation of S6 requires PKC

(**A**) D10 T cells were left unstimulated or were pretreated with vehicle, Akt*i*1/2, or BIM before being stimulated with biotinylated anti-CD3, anti-CD28, and anti-CD4 antibodies and streptavidin for 30 min. Cells were then analyzed by flow cytometry to detect pS6. (**B**) Primary murine T cells were left untreated or were pretreated with BIM before being stimulated with anti-CD3 and anti-CD28 antibodies for 30 min. Cells were then analyzed by flow cytometry for pS6. Graph shows mean MFIs of pS6 ± SEM of triplicate measurements from a single experiment and are representative of three independent experiments. $^{**}P < 0.01$, by unpaired Student's t-test. (**C**) Jurkat cells (top) and JPM 50.6 cells (bottom) were left untreated or were pretreated with the indicated concentrations of BIM before being stimulated with anti-CD3 and anti-CD28 antibodies for 15 min. Cells were then analyzed by flow cytometry for pS6. Right: Graphs show the fold-increase in mean fluorescence intensity (MFI) for each condition. Data are means ± SEM of three (Jurkat) and two (JPM 50.6) independent experiments.

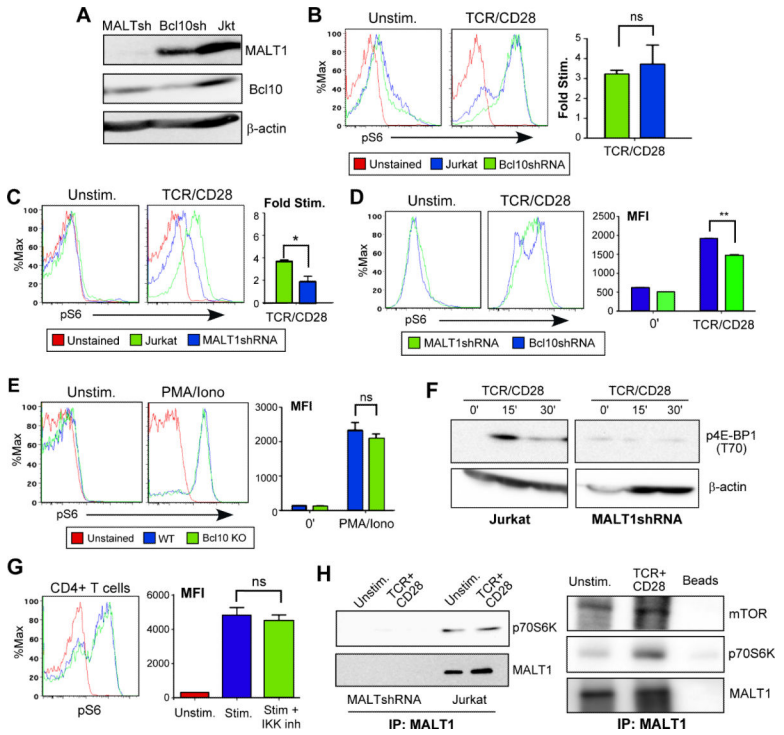

Fig. 4. MALT1, but not Bcl10, is required for optimal S6 phosphorylation in response to TCR and CD28 stimulation

(**A**) Parental Jurkat cells, MALT1shRNA cells, and Bcl10shRNA cells were analyzed by Western blotting with antibodies against the indicated proteins. Data are representative of three independent experiments. (**B** and **C**) Parental Jurkat cells (B) and either Bcl10shRNA cells (B) or MALT1shRNA cells (C) were stimulated with anti-CD3 and anti-CD28 antibodies for 15 min and then were analyzed by flow cytometry for pS6. Bar graphs show the fold-increase in pS6 in the indicated cells. Data are means ± SEM from three independent experiments. ns, not significant. (**D**) MALT1shRNA and Bcl10shRNA cells were stimulated with anti-CD3 and anti-CD28 antibodies for 15 min, before being analyzed by flow cytometry for pS6. The bar graph shows the fold-increase in pS6 in the indicated cells. Data are means ± SEM from three independent experiments. (**E**) Primary $CD4^+$ T cells from WT and Bcl10 KO mice were left untreated or were stimulated with PMA and ionomycin for 30 min before being analyzed by flow cytometry for pS6. The bar graph shows average MFIs for pS6 ± SEM of triplicate samples from one experiment, which is representative of three experiments. (**F**) Jurkat cells and MALT1shRNA cells were stimulated as indicated and then analyzed by Western blotting for p4E-BP1(T70). β-actin was used as a loading control. Blots are representative of three independent experiments. (**G**) Primary mouse $CD4^+$ T cells were left untreated or were pretreated with the IKK-2 inhibitor before being stimulated with anti-CD3 and anti-CD28 antibodies for 30 min, and then analyzed by flow cytometry for pS6. Bar graph shows mean MFIs for pS6 ± SEM of triplicate samples from one experiment, which is representative of two experiments. (**H**) Jurkat cells were left untreated or were stimulated with anti-CD3 and anti-CD28 antibodies before being subjected to immunoprecipitation (IP) with anti-MATL1 antibody. IP's were then analyzed by Western blotting to detect MALT1-associated S6K (left) and mTOR

(right). Blots are representative of three independent experiments. *$P < 0.05$, **$P < 0.01$, by unpaired student's t test.

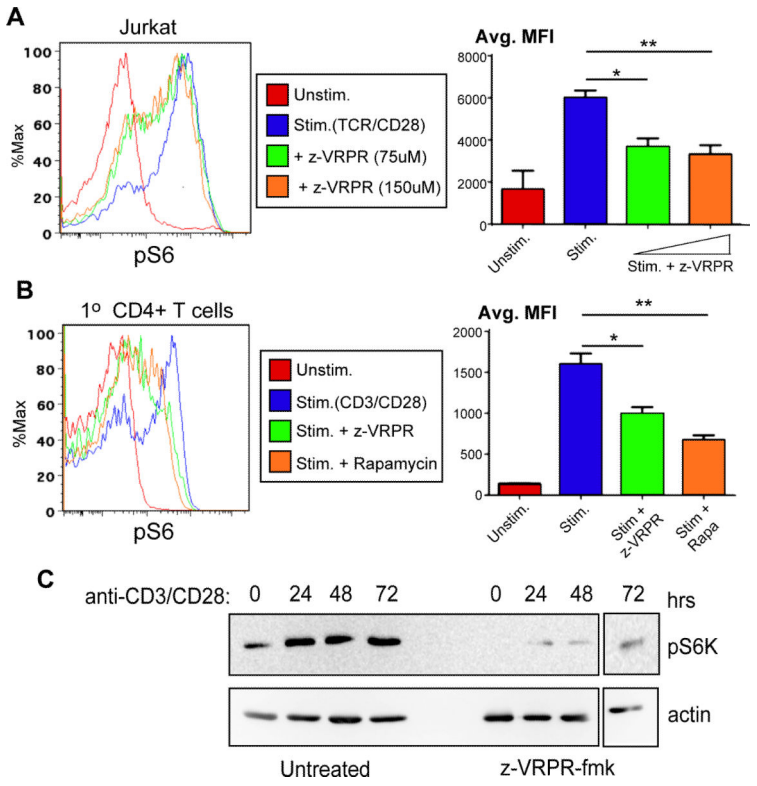

Fig. 5. The catalytic activity of MALT1 contributes to TCR- and CD28-stimulated phosphorylation of S6K and S6 in T cells

(**A** and **B**) Jurkat cells (A) and primary mouse $CD4^+$ T cells (B) were left untreated, were (A) pretreated with the indicated concentrations of z-VRPR-fmk, or were (B) pretreated with either z-VRPR-fmk or rapamycin before being stimulated with anti-TCR and anti-CD28 antibodies (Jurkat cells) or anti-CD3 and anti-CD28 antibodies (mouse $CD4^+$ T cells). (A and B) Cells were then analyzed by flow cytometry for pS6. Bar graph shows mean MFIs of pS6 ± SEM from (A) three independent experiments or (B) triplicate measurements from a single experiment, which is representative of three independent experiments. $*P < 0.05$, $**P < 0.01$, by unpaired student's t test. (**C**) Primary mouse $CD4^+$ T cells were left untreated or were stimulated with anti-CD3 and anti-CD28 antibodies for indicated times. Cell lysates were then analyzed by Western blotting for p70S6K (top) or β-actin (bottom). Blots are representative of three independent experiments.

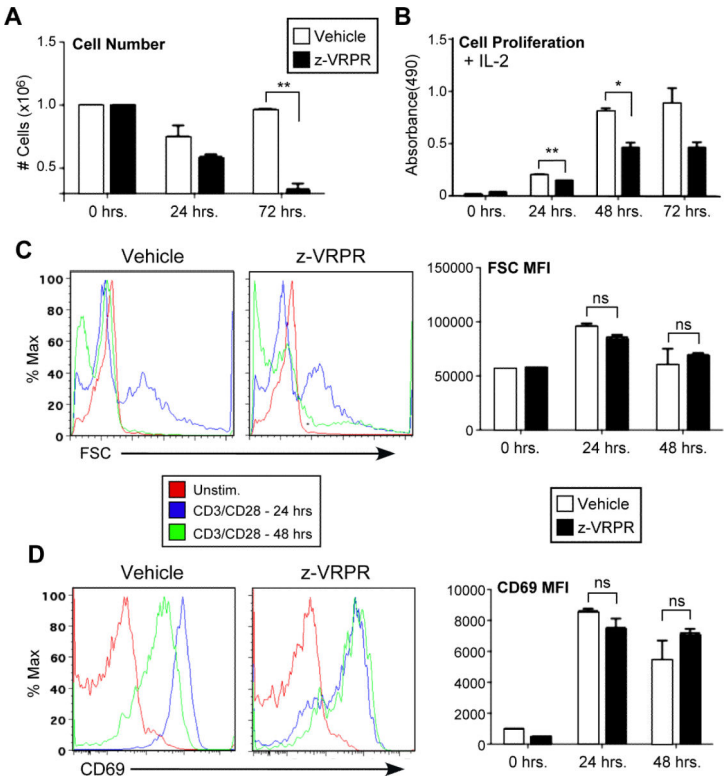

Fig. 6. MALT1 activity is required for T cell proliferation, but not for acute blasting or early activation

(**A**) Primary mouse $CD4^+$ T cells were pretreated with vehicle or z-VRPR-fmk before being stimulated with anti-CD3 and anti-CD28 antibodies for the indicated times. Numbers of live cells were determined by trypan blue exclusion. Data are means ± SEM of three independent experiments. $^{**}P < 0.01$, by unpaired student's t test. (**B**) Primary mouse $CD4^+$ T cells pretreated with either vehicle or inhibitor in the presence of exogenous IL-2 were stimulated with anti-CD3 and anti-CD28 antibodies for the indicated times and then cell proliferation was assessed by MTT assay. Data are means ± SEM of three independent experiments. $^{*}P < 0.05$; $^{**}P < 0.01$, by unpaired student's t test. (**C**) Primary mouse $CD4^+$ T cells were pretreated with vehicle or z-VRPR-fmk, stimulated for the indicated times, and then analyzed by flow cytometry for forward scatter (FSC), an indicator of cell size. Bar graph shows mean FSC values ± SEM of vehicle- and inhibitor-treated cells from three experiments. ns, not significant. (**D**) Mouse $CD4^+$ T cells were pretreated with vehicle or z-VRPR-fmk before being stimulated with anti-CD3 and anti-CD28 antibodies for the indicated times, and then were analyzed for cell-surface abundance of CD69 by flow cytometry. Bar graph shows mean CD69 MFI values ± SEM of vehicle- and inhibitor-treated cells for the indicated times from three experiments.

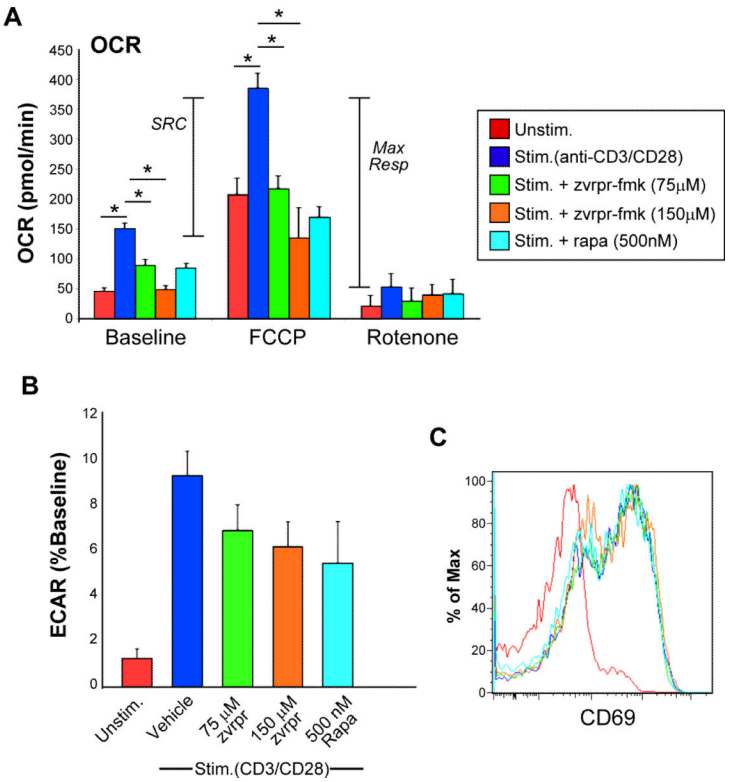

Fig. 7. MALT1 activity is required for TCR-dependent changes in T cell metabolism

(**A** and **B**) Naïve CD4$^+$ T cells were isolated from C57BL/6 mice, pretreated with vehicle or the indicated inhibitors, and stimulated with anti-CD3 and anti-CD28 antibodies. After 24 hours, cells were analyzed on a Seahorse XF24 analyzer to determine (A) oxygen consumption rate (OCR) and (B) extracellular acidification rate (ECAR), which are measures of oxidative phosphorylation and glycolysis, respectively. Spare respiratory capacity (SRC) refers to the amount of additional ATP (above baseline) that can be produced by mitochondria in the presence of the ionophore uncoupling agent FCCP. The maximal respiratory capacity ("Max Resp") is determined by the difference between the response to FCCP and complete inhibition of the electron transport chain by rotenone. *P < 0.05, by unpaired student's t test. (**C**) After Seahorse analysis, the cells shown in (A) and (B) were analyzed by flow cytometry to determine the relative cell-surface abundance of CD69 on the indicated cells. Data are representative of three independent experiments.

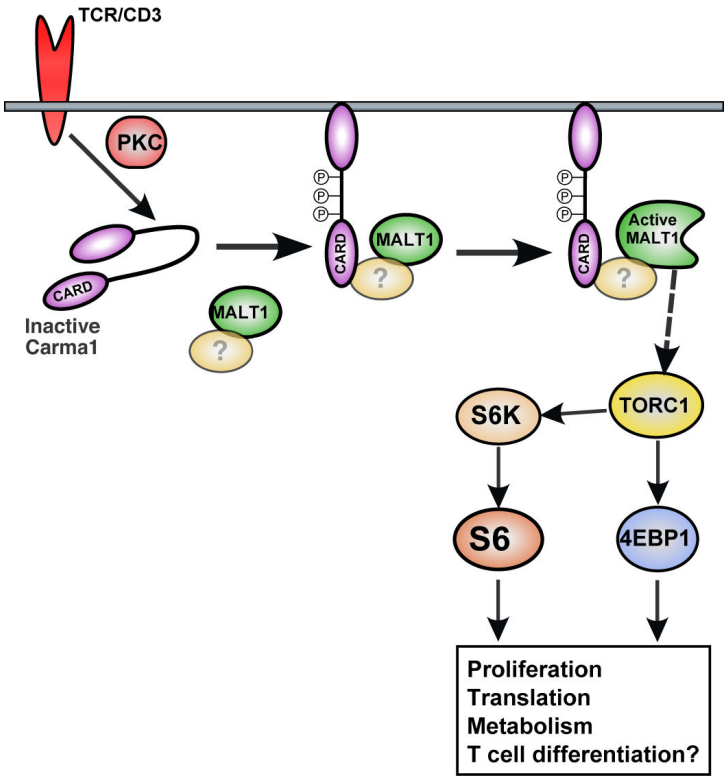

Fig. 8. Model for the regulation of mTOR signaling by Carma1 and MALT1 in response to TCR signaling in T cells

Our data suggest that Carma1 and MALT1 participate in the TCR-dependent activation of mTOR downstream of PKC. The other CBM component, Bcl10, seems to be dispensable for this pathway, although it is possible that another protein substitutes for Bcl10 in mediating an association between Carma1 and MALT1 (indicated by the oval with a question mark). See the Discussion for more details.